Determination of homogeneity of pure and doped lithium niobate by second harmonic generation temperature phase matching

Chr. a. d. Horst, K.-U. Kasemir, and K. Betzler[a)]
Fachbereich Physik, Universität Osnabrück, Barbarastrasse 7, D-49069 Osnabruck, Germany

(Received 13 July 1998; accepted for publication 10 August 1998)

Employing a comprehensive Sellmeier equation for the refractive indices, we derive calibration curves to be used for the homogeneity characterization of lithium niobate. Applying the calculated results, *quantitative* homogeneity parameters can be derived from temperature tuning curves for noncritical second harmonic generation, which are usually measured to state the composition of the material. The calibration method is of interest and presently is being used for pure as well as Mg-, Zn-, and In-doped crystals in the whole concentration regime. © *1998 American Institute of Physics.* [S0021-8979(98)08321-2]

I. INTRODUCTION

For many electro-optic and nonlinear optical applications, lithium niobate ($LiNbO_3$) is one of the most interesting materials currently available; for a recent review see Ref. 1. Its physical properties can be tuned by varying the composition and adding dopants. Postgrowth vapor transport equilibration (VTE) can be used to modify the lithium-to-niobium ratio of homogeneous samples, which are grown most conveniently from congruent melts. To check the homogeneity, which is a crucial parameter for most applications, means of characterization become increasingly important for the professional development of $LiNbO_3$ devices.

A thorough analysis of methods for the characterization of $LiNbO_3$ has shown that optical methods offer excellent accuracy and are also most convenient to use.[2] Procedures based on second harmonic generation (SHG) offer superior relative and absolute sensitivities. While these techniques can be extended to provide spatially resolved two- or even three-dimensional composition scans,[3] it is known that simply measuring the tuning curve for noncritical phase matching as a function of temperature or wavelength is often sufficient to rank similar crystals according to their relative homogeneity.

Based on numerical calculations, we will extend this method to allow absolute quantitative measurements of crystal homogeneity.

II. PRINCIPLES OF THE METHOD

The SHG intensity I_{SHG} can be written as

$$I_{SHG} \sim \left(I_0 L \frac{\sin(\Delta k L/2)}{\Delta k L/2} \right)^2 \tag{1}$$

for fundamental wavelength λ with intensity I_0, phase mismatch $\Delta k = 4\pi(n_\lambda - n_{\lambda/2})/\lambda$, and crystal length L.

The refractive indices $n_{\lambda,\lambda/2}$ and hence Δk depend on temperature, wavelength, and crystal composition. Early approaches tried to fit polynomial expressions to measured indices of refraction.[4] Schlarb and Betzler proposed a generalized Sellmeier equation permitting calculation of refractive indices for $LiNbO_3$ as a function of wavelength, temperature, and lithium content.[5] It was soon extended to describe $LiNbO_3$ doped with Mg,[6] Zn,[7] as well as In.[8]

SHG tuning curves for noncritical phase matching (PM) can be measured as a function of either temperature[9] or wavelength,[10] keeping the other parameter fixed. Due to the optical properties of $LiNbO_3$, the predominantly applied method is temperature tuning using a Nd:YAG laser at a fixed fundamental wavelength of 1064 nm. Consequently, we will restrict our considerations and calculations.

I_{SHG} reaches a maximum if $\Delta k(T)$ vanishes, i.e., when T reaches T_{pm}. For undoped $LiNbO_3$, T_{pm} is found to be about 0 °C for $c_{Li} = 48.4$ mol % Li_2O and close to 260 °C for $c_{Li} = 50$ mol % Li_2O.

In homogeneous materials oscillations of I_{SHG} can be observed for $T \neq T_{pm}$, particularly a periodic reduction to 0 as shown in Fig. 1. The absolute maximum at $T = T_{pm}$, however, is much more pronounced than the side maxima, so even in materials of uniform composition the minima cannot always be seen clearly because of signal noise. The same effect hampers the usability of tests based on the separation between adjacent minima and maxima, the height of the first subsidiary satellite relative to the central peak, or good zeros.

Therefore ΔT_{pm}, the observed full width at half maximum (FWHM) of the harmonic power near T_{pm}, is often used as an easily obtainable criterion for crystal homogeneity.[11] Harmonic power drops to 50% for $\Delta k L/2 \approx 1.392$, thus

$$\Delta T_{pm} \approx \frac{1.392\lambda}{\pi L} \left| \frac{\partial(n_\lambda - n_{\lambda/2})}{\partial T} \right|^{-1}_{T=T_{pm}} \tag{2}$$

assuming a linear dependence of Δk on T. Any deviations from linearity will perturb the results, mainly those obtained for small L, where the central peak of I_{SHG} extends over a wide temperature range.

As Nash *et al.*[12] deduced from calculations for undoped $LiNbO_3$, the broadening of ΔT_{pm} in inhomogeneous crystals is influenced by the way in which the constituents vary as a

[a)]Electronic mail: Klaus.Betzler@Uni-Osnabrueck.DE

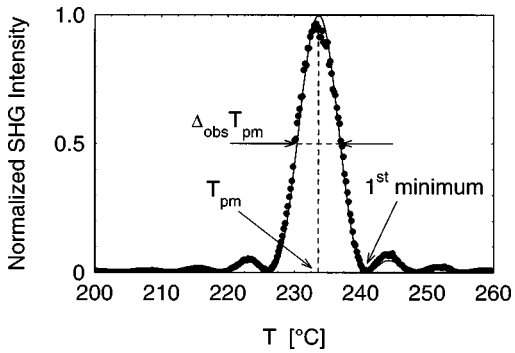

FIG. 1. Temperature-dependent SHG intensity of a VTE-treated $LiNbO_3$ crystal with 49.8 mol % Li_2O, 0.95 mm long, fundamental wavelength 1064 nm. Dots represent measured intensity, solid line calculated according to Eq. (1).

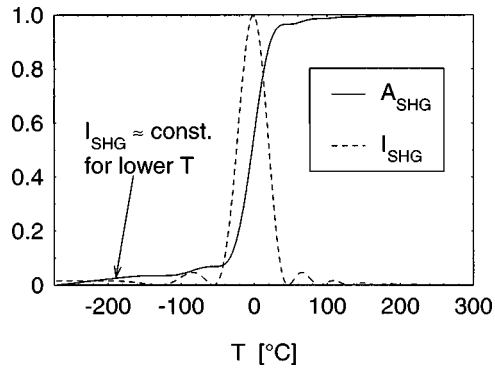

FIG. 2. Normalized simulated second harmonic intensity I_{SHG} and area thereunder A_{SHG} for $LiNbO_3$ with $c_{Li}=48.4$ mol % Li_2O, crystal length 0.2 mm.

function of crystal position, e.g., step-like, linear, Gaussian etc. An effective width, defined via the total area under the SHG tuning curve as

$$\Delta T^{\star}_{pm}=\frac{I_{SHG}(T)dT}{I_{SHG}(T_{pm})} \tag{3}$$

proved to be independent of the model used and should be preferred at least for strongly inhomogeneous samples.

For pure $LiNbO_3$, both ΔT_{pm} and $\Delta T^{\star}_{pm}$ can be approximated by curves based on ''stretched exponentials''

$$(\Delta T_{pm}L)(c_{Li})\approx A+Be^{-(c_{Li}-C)^D} \tag{4}$$

with only four adjustable parameters for $c_{Li} \in [48.4\cdots 50.0]$ mol % Li_2O and $L\in[0.1\cdots 10.0]$ mm.

A. Observed width

The derivative of the SHG birefringence versus temperature in Eq. (2) can be evaluated by means of the generalized Sellmeier equation for lithium niobate.[5] Equation (2) can then be approximated by Eq. (4) with reasonable accuracy using the fit parameters listed in Table I. Maximal relative deviations from ΔT_{pm} are smaller than 10^{-3} for $L \geqslant 0.33$ mm and still below 10^{-2} for $L\geqslant 0.11$ mm. As an effect observable only at low c_{Li} (corresponding to low T_{pm}), the product $\Delta T_{pm}L$ tends to grow slightly for decreasing L instead of remaining constant. The reason for this is the nonlinear temperature dependence of Δk which shows up more remarkably for larger ΔT_{pm}.

B. Effective width

From a mathematical point of view, the integral in Eq. (3) should be calculated from $-\infty$ to ∞. Using the Sellmeier equation we could extend our numerical simulations from $T=0$ K up to temperatures T where $I_{SHG}(T)$ falls below machine precision. The experimentally accessible temperature interval, however, is usually further limited, yielding smaller integrals in Eq. (3).

Moreover, the disappearing first derivative of $\Delta k(T)$ for low temperatures leads to a constant $I_{SHG}(T)$ for a large temperature interval as shown in Fig. 2. Most pronounced in the case of thin crystals or for small c_{Li}, $\Delta T^{\star}_{pm}(c_{Li})L$ tends to oscillate with c_{Li} and L. Depending on whether the integration at low T extends over a broadened minimum or side maximum of I_{SHG}, the error in $\Delta T^{\star}_{pm}L$ might be up to 3% for the example given in Fig. 2.

Nash *et al.* did not observe this problem because of their linear assumption for $\Delta k(T)$. By choosing $T=-200$ °C as a lower integration limit, we tried to minimize these oscillations while still matching common experimental temperature ranges.

Consequently, the fit accuracy of Eq. (4) decreases for very small crystals. Relative deviations, which are well below 10^{-3} for $L\geqslant 2$ mm, approach 10^{-2} for $L\cong 0.5$ mm.

TABLE I. Fit parameters.

Parameter	ΔT_{pm}	$\Delta T^{\star}_{pm}$
A	2.8080	2.6550
B	11.625	14.530
C	48.103	48.098
D	0.3694	0.3345

III. RESULTS

When comparing nominally equivalent crystals, the most homogeneous specimen can easily be detected as the one

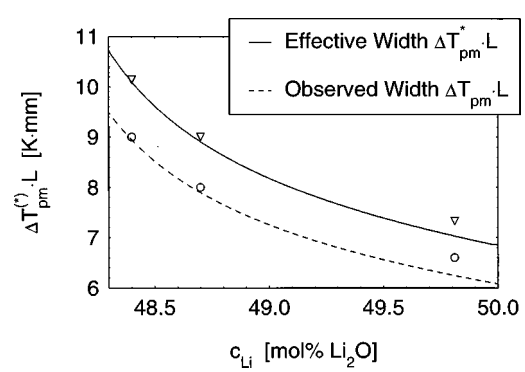

FIG. 3. Observed and effective width of phase-matching temperature as a function of crystal composition for pure $LiNbO_3$, curves calculated using the generalized Sellmeier equation for homogeneous material; markers represent our experimental data.

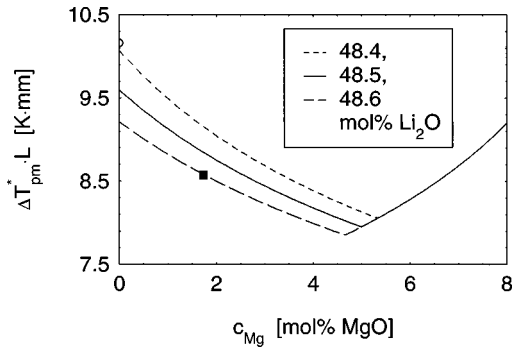

FIG. 4. Effective width of phase-matching temperature ($\Delta T^{\star}_{\mathrm{pm}}L$) as a function of dopant concentration for Mg-doped $LiNbO_3$. The dot indicates the measured value from Ref. 11.

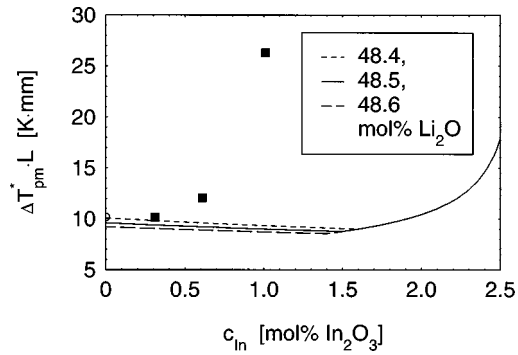

FIG. 6. Effective width $\Delta T^{\star}_{\mathrm{pm}}L$ as a function of In concentration in $LiNbO_3$. Dots indicate measured values for several samples.

yielding the smallest $\Delta T^{\star}_{\mathrm{pm}}$ or ΔT_{pm}. For ranking samples of different length L, the widths ΔT must be normalized by multiplying with the length according to

$$(\Delta T^{\star}_{\mathrm{pm}}L)_{\mathrm{i}} \Leftrightarrow (\Delta T^{\star}_{\mathrm{pm}}L)_{\mathrm{k}}, \tag{5}$$

where indices i and k denote the respective sample. Of course one has to bear in mind the precision limitations discussed in previous sections, i.e., slight deviations for small samples.

In the absence of comparable reference crystals with the same composition and dopant concentration, or when a more quantitative analysis is required, it becomes necessary to calculate $\Delta T^{\star}_{\mathrm{pm}}$ or rather the size-independent product $\Delta T^{\star}_{\mathrm{pm}} \cdot L$ for an ideal sample from the refractive indices. This can be accomplished only numerically, using the Sellmeier description for the refractive indices.

A. Undoped $LiNbO_3$

Figure 3 shows calculated curves for the ideal observed and effective widths for undoped $LiNbO_3$ with a lithium content ranging from 48.3% to 50.0%. Undoped $LiNbO_3$ is usually grown with rather good homogeneity so each of the width values discussed can be used for characterization. This is verified by a comparison with the experimental data from different samples. The rankings via observed and effective width both yield the same results: The crystals grown near the congruently melting composition exhibit better homogeneity than the crystals near the stoichiometric composition. A simple direct comparison of the width values of the individual crystals would—as a mistake—have proved the opposite. This emphasizes the necessity for calculated reference curves.

B. Doped $LiNbO_3$

As doped $LiNbO_3$ crystals usually are less homogeneous than undoped ones, the effective width will be a better measure in this field. We therefore concentrate on the effective width despite the slightly higher experimental effort to measure it.

The calculated dependences as a function of dopant concentration for Mg, Zn, and In are shown in Figs. 4, 5, and 6, respectively. Doped $LiNbO_3$ is usually grown from a congruent melt. Because exact definitions of congruency vary slightly among authors, we choose a range of lithium concentrations from 48.4 to 48.6 mol % Li_2O for doped material. Considering this variation, previously published data for Mg doped crystals[11] do attest to rather uniform crystal composition.

For all of the considered dopants, the calculated ideal $\Delta T^{\star}_{\mathrm{pm}} \cdot L$ shows a decrease with rising dopant concentration up to a certain threshold[13] followed by an increase in further rising concentration.

Characterizing a set of recently grown In doped[8] crystals we observed a steep increase in the deviation between measured $\Delta T^{\star}_{\mathrm{pm}}L$ and ideal values (Fig. 6). For these samples, this must be explained as an increase of inhomogeneity with

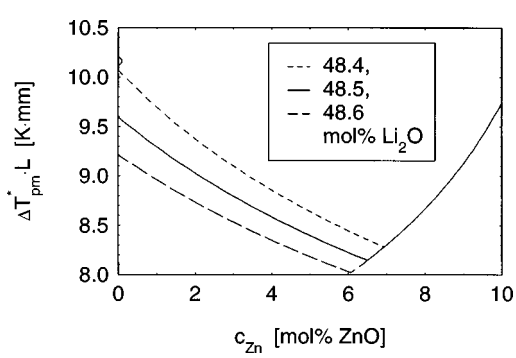

FIG. 5. Effective width $\Delta T^{\star}_{\mathrm{pm}}L$ as a function of Zn concentration in $LiNbO_3$.

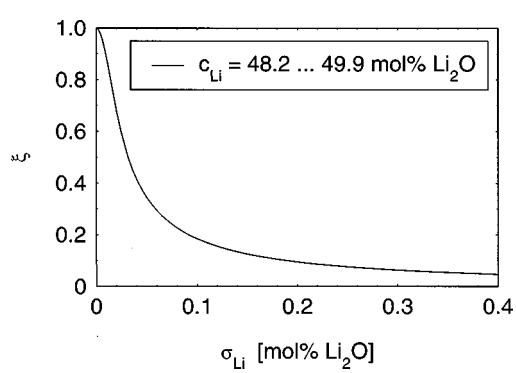

FIG. 7. Calculated quality parameter ξ for pure $LiNbO_3$ as a function of assumed variation σ, valid for 48.2–49.9 mol % Li_2O.

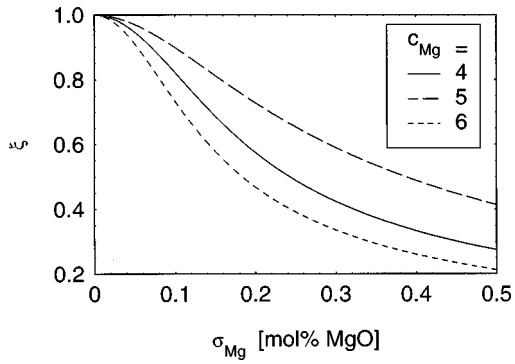

FIG. 8. Calculated quality parameter ξ for Mg-doped $LiNbO_3$ as a function of assumed variation σ, $c_{Li}=48.5$ mol % Li_2O, concentration of dopant c_{Mg} in mol % MgO.

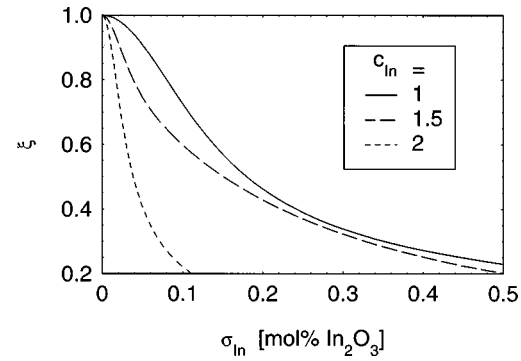

FIG. 10. Quality parameter ξ for $LiNbO_3$:In ($c_{Li}=48.5$ mol % Li_2O) calculated as a function of assumed variation σ for selected mol % In_2O_3 (c_{In}).

the further addition of In_2O_3, emphasizing the well known difficulty of growing $LiNbO_3$:In of high optical quality.[14]

C. Quantitative homogeneity criterion

In the deviation of the measured real effective width from the calculated ideal one can only serve as a *qualitative* measure to rank crystals. To use it as a *quantitative* measure we developed calibration curves which relate this deviation to a corresponding inhomogeneity of Li content or dopant concentration.

As a means of comparison for inhomogeneous crystals we define a quality parameter $\xi \in [0 \cdots 1]$:

$$\xi := \frac{(\Delta T^{\star}_{pm} L)_{ideal}}{(\Delta T^{\star}_{pm} L)_{real}}. \tag{6}$$

Assuming a Gaussian normal distribution for the concentration c_X of $X=Li$, Mg, Zn, or In with standard deviation σ, we calculated the weighted superposition of the resulting SHG intensities as a function of temperature:

$$I_{\sigma}(c_X,T) = \frac{1}{\sqrt{2\pi\sigma^2}} \times \int \exp\left[-\frac{1}{2}\left(\frac{c-c_X}{\sigma}\right)^2\right] I_{SHG}(c,T)\,dc. \tag{7}$$

The $\Delta T^{\star}_{pm}$'s of these curves were inserted for $(\Delta T^{\star}_{pm} L)_{real}$ into Eq. (6) to obtain a simulation of imperfect crystals.

The relationship between the quality parameter ξ and the size of the standard deviation σ is shown in Figs. 7–10.

For undoped $LiNbO_3$ (Fig. 7), a single universal calibration curve is valid for the whole concentration range of interest.

In doped $LiNbO_3$, most of the physical parameters change their behavior at the so called threshold concentration of the dopant. This threshold concentration tends to be approximately 5 mol % MgO,[15] 6.5 mol % ZnO,[16] and 1.5 mol % In_2O_3,[17] respectively, for congruently grown doped $LiNbO_3$. In view of this fact, for each of the regarded dopants three calibration curves—for the concentration ranges below, around and above the threshold, respectively—are obtained (Figs. 8–10).

Special care must be taken for concentrations near this peculiar threshold c_t. As Fig. 11 shows for $LiNbO_3$:Mg, T_{pm} reaches a maximum at c_t. Consequently all deviations $\sigma_{Mg}>0$ result in a diminution of the measured value for T_{pm}. The same effect tends to tighten $I_{\sigma}(c_X,T)$ near c_t. The parameter ξ is raised accordingly, pretending improved crystal quality except for the case of In, where the strong decrease of ξ with σ_{In} for concentrations $c_{In}>c_t$ seems to compensate for this effect.

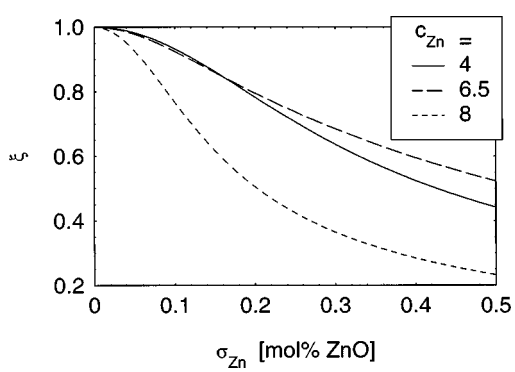

FIG. 9. Calculated quality parameter ξ for $LiNbO_3$ doped with different molar concentrations c_{Zn} of ZnO as a function of assumed variation σ, $c_{Li}=48.5$ mol % Li_2O.

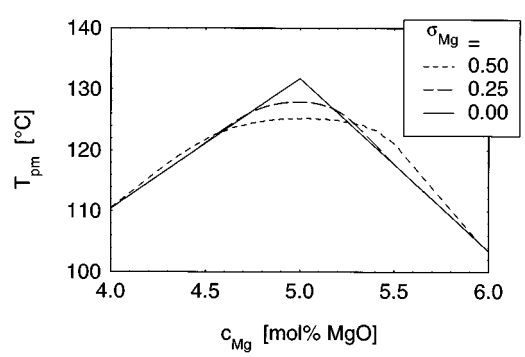

FIG. 11. Phase-matching temperature T_{pm} for congruent $LiNbO_3$:Mg for different σ_{Mg}, based on the proposed simple model for inhomogeneous materials.

To characterize a sample, one has to calculate the quality parameter ξ using the measured real effective width and the ideal one given in Figs. 3–6. Applying the respective calibration curve, ξ then can be directly related to the concentration distribution in the sample.

Applying this procedure to the above mentioned In-doped crystals with 0.3, 0.6, and 1 mol % In_2O_3 from the declining quality parameters $\xi = 0.93$, 0.76, and 0.34 we can state variations of c_{In} by $\sigma_{In} = 0.05$, 0.1, and 0.3 mol % In_2O_3. Likewise the obtained ξ could originate from Li variations $\sigma_{Li} = 0.009$, 0.017, and 0.05 mol % Li_2O. Together, both values for each sample can be regarded as a combined upper limit for the concentration inhomogeneities.

IV. CONCLUSION

Measuring $\Delta T_{pm}L$ offers an easy way to rank crystals with nominally similar properties. The effective width value $\Delta T^{\star}_{pm}L$ is better suited for crystals of arbitrary homogeneity, and a fit for both ΔT_{pm} and $\Delta T^{\star}_{pm}$ in undoped $LiNbO_3$ and for $\Delta T^{\star}_{pm}$ in doped $LiNbO_3$ is given. To spare tedious calculations based on the more precise Sellmeier equation, the graphed quality parameters ξ for pure as well as doped $LiNbO_3$ might prove useful. Deviations from exact homogeneity can be detected by measuring the effective width and relating it to the ideal one and can be quantitatively evaluated using the calibration curves given. Deconvoluting the SHG intensity as measured with nonuniform samples thus allows one to find a bracketing interval for the Li content or dopant concentrations in lithium niobate.

ACKNOWLEDGMENT

Financial support from the Deutsche Forschungsgemeinschaft (Grant No. SFB 225) is gratefully acknowledged.

[1] IEEE J. Quantum Electron. **33**, (1997).
[2] M. Wöhlecke, G. Corradi, and K. Betzler, Appl. Phys. B: Lasers Opt. **63**, 323 (1996).
[3] A. Reichert and K. Betzler, J. Appl. Phys. **95**, 2209 (1996).
[4] G. D. Boyd, V. L. Bond, and H. L. Carter, J. Appl. Phys. **38**, 1941 (1967).
[5] U. Schlarb and K. Betzler, Phys. Rev. B **48**, 15613 (1993).
[6] U. Schlarb and K. Betzler, Phys. Rev. B **50**, 751 (1994).
[7] U. Schlarb, M. Wöhlecke, B. Gather, A. Reichert, K. Betzler, T. Volk, and N. Rubinina, Opt. Mater. **4**, 791 (1995).
[8] K. Kasemir, K. Betzler, B. Matzas, B. Tiegel, M. Wöhlecke, N. Rubinina, and T. Volk, Phys. Status Solidi A **166**, R7 (1998).
[9] R. L. Byer, J. F. Young, and R. S. Feigelson, J. Appl. Phys. **41**, 2320 (1970).
[10] T. Pliska, F. Mayer, D. Fluck, P. Günter, and D. Rytz, J. Opt. Soc. Am. B **12**, 1878 (1995).
[11] J.-S. Lee, B. K. Rhee, C.-D. Kim, and G.-T. Joo, Mater. Lett. **33**, 63 (1997).
[12] F. R. Nash, G. D. Boyd, M. S. III, and P. M. Bridenbaugh, J. Appl. Phys. **41**, 2564 (1970).
[13] T. Volk, M. Wöhlecke, A. Reichert, F. Jermann, and N. Rubinina, Ferroelectr. Lett. Sect. **20**, 97 (1995).
[14] T. Volk, M. Wöhlecke, N. Rubinina, N. Razumovski, F. Jermann, C. Fischer, and R. Böwer, Appl. Phys. A: Mater. Sci. Process. **60**, 217 (1994).
[15] D. A. Bryan, R. Gerson, and H. E. Tomaschke, Appl. Phys. Lett. **44**, 847 (1984).
[16] T. R. Volk and N. M. Rubinina, Fiz. Tverd. Tela (Leningrad) **33**, 1192 (1991).
[17] T. R. Volk and N. M. Rubinina, Ferroelectr. Lett. Sect. **14**, 37 (1992).